

SCALING LAW OF RELATIVISTIC SWEET–PARKER TYPE MAGNETIC RECONNECTION

HIROYUKI R. TAKAHASHI¹

Center for Computational Astrophysics, National Astronomical Observatory of Japan, 2-21-1, Osawa, Mitaka, Tokyo 181-8588, Japan

TAKAHIRO KUDOH²

Division of Theoretical Astronomy, National Astronomical Observatory of Japan, 2-21-1, Osawa, Mitaka, Tokyo 181-8588, Japan

YOUHEI MASADA³

Department of Computational Science, Kobe University, 1-1 Rokkodai, Nada, Kobe 657-8501, Japan

AND

JIN MATSUMOTO⁴

Kwasan and Hida Observatories, Graduate School of Science, Kyoto University, Kyoto 607-8471, Japan

submitted to ApJ Letter

ABSTRACT

Relativistic Sweet–Parker type magnetic reconnection is investigated by relativistic resistive magnetohydrodynamic (RRMHD) simulations. As an initial setting, we assume anti-parallel magnetic fields and a spatially uniform resistivity. A perturbation imposed on the magnetic fields triggers magnetic reconnection around a current sheet, and the plasma inflows into the reconnection region. The inflows are then heated due to ohmic dissipation in the diffusion region, and finally become relativistically hot outflows. The outflows are not accelerated to ultra-relativistic speeds (i.e., Lorentz factor $\simeq 1$), even when the magnetic energy dominates the thermal and rest mass energies in the inflow region. Most of the magnetic energy in the inflow region is converted into the thermal energy of the outflow during the reconnection process. The energy conversion from magnetic to thermal energy in the diffusion region results in an increase in the plasma inertia. This prevents the outflows from being accelerated to ultra-relativistic speeds. We find that the reconnection rate \mathcal{R} obeys the scaling relation $\mathcal{R} \simeq S^{-0.5}$, where S is the Lundquist number. This feature is the same as that of non-relativistic reconnection. Our results are consistent with the theoretical predictions of Lyubarsky (2005) for Sweet–Parker type magnetic reconnection.

Subject headings: magnetic fields – magnetic reconnection – magnetohydrodynamics (MHD) – relativistic processes

1. INTRODUCTION

Magnetic reconnection is one of the most important subjects in the studies of space, laboratory, and astrophysical plasmas (Biskamp 1986; Priest & Forbes 2000). In particular, it plays an essential role in the understanding of energy conversion processes in high energy plasmas that characterize astrophysical compact objects, such as neutron stars (Kennel & Coroniti 1984; Lyubarsky & Kirk 2001; Lyubarsky 2003), soft gamma-ray repeaters (Lyutikov 2006; Gill & Heyl 2010; Masada et al. 2010), active galactic nuclei (Di Matteo 1998), and gamma-ray bursts (Drenkhahn 2002; McKinney & Uzdensky 2010; Zhang & Yan 2011).

While issues concerning the physical mechanisms and properties of magnetic reconnection remain unsettled in the relativistic regime, a few theoretical studies of relativistic effects have been made (Blackman & Field 1994; Lyutikov & Uzdensky 2003; Lyubarsky 2005; Tolstykh et al. 2007; Tenborge et al. 2010). Lyutikov & Uzdensky (2003) studied relativistic Sweet–Parker type reconnection within the framework of magnetohydrodynamics (MHD), finding that the reconnection-driven outflow can have an ultra-relativistic

speed (Lorentz factor $\gamma \gg 1$) when the magnetic energy is preferentially converted to kinetic energy. They concluded that the reconnection rate would be enhanced in the relativistic regime due to Lorentz contraction. In contrast, Lyubarsky (2005) concluded that the outflow cannot be accelerated to a relativistic speed ($\gamma \simeq 1$) because the magnetic energy should be converted into thermal energy to maintain the pressure balance across the current sheet. The effect of the Lorentz contraction is then negligible and the reconnection rate would not be enhanced.

Recently, further numerical studies have been conducted on relativistic magnetic reconnection. Particle-in-cell simulations are mainly employed to ascertain the reconnection mechanism in the collisionless regime without introducing a phenomenological parameter, i.e., electric resistivity (Zenitani & Hoshino 2001; Jaroschek et al. 2004; Zenitani & Hoshino 2007; Zenitani & Hesse 2008a; Bessho & Bhattacharjee 2007; Zenitani & Hesse 2008b). Watanabe & Yokoyama (2006) studied Petschek type relativistic magnetic reconnection for the first time in a spatially localized resistivity model using relativistic resistive magnetohydrodynamic (RRMHD) simulations. Relativistic two-fluid MHD simulations were performed by Zenitani et al. (2009a,b). Zenitani et al. (2010) nu-

TABLE 1
LIST OF SIMULATION RUNS

model	β_0	σ_0	$u_{A,0}$	R_M	γ_{\max}	$\tilde{M}_{A,\max}$	t_{20}	$(1+h+\sigma) _{\text{in}}$	σ_{out}	h_{out}	γ_{out}
B1R2	0.1	20	2.00	200	5.0	2.45	191.4	22.7	1.86×10^{-2}	33.7	1.40
B2R2	0.2	10	1.41	200	3.0	2.00	195.1	13.8	6.58×10^{-3}	18.7	1.29
B4R2	0.4	5	1.00	200	2.0	1.73	206.5	9.36	2.22×10^{-3}	11.1	1.17
B8R2	0.8	2.5	0.71	200	1.5	1.58	233.3	7.15	8.27×10^{-4}	7.48	1.08
B2R1	0.2	10	1.41	100	3.0	2.00	290.7	13.4	9.56×10^{-3}	19.5	1.20
B2R5	0.2	10	1.41	500	3.0	2.00	157.6	14.1	2.21×10^{-3}	13.9	1.28
B2R10	0.2	10	1.41	1000	3.0	2.00	151.9	14.4	1.00×10^{-3}	9.91	1.22

NOTE. — Columns: (6) possible maximum outflow Lorenz factor evaluated from equation (6); (7) $\tilde{M}_{A,\max} \equiv u_{\max}/u_{A,0}$; (8) time at which the current sheet length reaches $Y = 20 \equiv L_{20}$; (9) the total specific enthalpy evaluated at $(X, Y) = (5, 0)$ when $t = t_{20}$; (10)-(12) the magnetization parameter, the specific enthalpy, and the Lorentz factor evaluated at $(X, Y) = (0, L_{20})$ when $t = t_{20}$.

merically examined relativistic magnetic reconnection using various resistivity models and obtained Petschek and Sweet–Parker type magnetic reconnection in relativistic plasmas.

While these previous studies have revealed much about Petschek type reconnection in the regime of low magnetic Reynolds number, $R_M \lesssim 160$, the physics of Sweet–Parker type magnetic reconnection and the dependence of the reconnection rate on the magnetic Reynolds number remain unsolved. In this Letter, we focus on Sweet–Parker type magnetic reconnection and investigate the basic properties through RRMHD simulations. This is the first systematic study of relativistic Sweet–Parker type magnetic reconnection for a broad range of magnetic Reynolds number $R_M \leq 10^3$.

2. NUMERICAL MODEL

We numerically solve a set of RRMHD equations in two-dimensional Cartesian coordinates (X, Y) with the simple form of Ohm’s law,

$$\mathbf{j} = q\mathbf{v} + \eta^{-1}\gamma[\mathbf{E} + \mathbf{v} \times \mathbf{B} - (\mathbf{E} \cdot \mathbf{v})\mathbf{v}], \quad (1)$$

where q , \mathbf{j} , η , \mathbf{v} , γ , \mathbf{E} , \mathbf{B} are the charge density, electric current, electric resistivity, three velocity, Lorentz factor, electric field, and magnetic field, respectively. We set the light speed, Boltzmann constant, and average particle mass as unity throughout this paper.

The relativistic Harris sheet is adopted as an initial setting (Kirk & Skjæraasen 2003). The spatial distribution of the magnetic field is then given by $B_x(X, Y) = B_z(X, Y) = 0$ and $B_y(X, Y) = B_0 \tanh(2X/\lambda)$, where B_0 is the field strength of the sheath plasma ($X \rightarrow \pm\infty$) and λ is the initial thickness of the current sheet. The gas pressure and density profiles are determined by the local pressure balance, i.e. $p = p_0 + [B_0^2 - B_y^2(X, Y)]/(8\pi)$ and $\rho = p/T_0$, where p_0 is the initial gas pressure of the sheath plasma and T_0 is the initial plasma temperature, which is assumed to be constant throughout the region. We set $p_0 = T_0 = 1$ and fix the specific heat ratio Γ as $\Gamma = 4/3$ throughout this paper. The magnetic reconnection is triggered around the origin by a perturbation of the magnetic field described in vector potential form as $\delta A_z = -\delta B_0 \lambda \exp[-(X^2 + Y^2)/\lambda^2]$, where $\delta B_0 = 0.03B_0$ is the amplitude of the perturbation.

The plasma β in the sheath is defined as $\beta_0 \equiv 8\pi p_0/B_0^2$. The magnetization parameter corresponding to each model is $\sigma_0 = 20, 10, 5, 2.5$, where $\sigma \equiv B^2/(4\pi\rho\gamma^2)$ and a subscript “0” denotes a quantity of the sheath

plasma. The corresponding Alfvén four speed is $u_{A,0} \equiv v_{A,0}/\sqrt{1-v_{A,0}^2} = 2.0, 1.41, 1.0, 0.71$, where v_A is the Alfvén speed. In our models, the electric resistivity is assumed to be uniform. We vary the resistivity η for magnetic Reynolds number $R_M \equiv 4\pi\lambda/\eta = 100, 200, 500, 1000$. We note that R_M defined by the full thickness of the initial current sheet is twice as large as that used in the previous study by Zenitani et al. (2010) who defined R_M by the half thickness of the current sheet. The parameters adopted in each model are summarized in Table 1.

The two-dimensional calculation is performed in the X – Y plane with a volume bounded by $X = [0, 50]$ and $Y = [0, 75]$. The length and time are normalized by the initial thickness of the current sheet λ and its Alfvén crossing time $\tau_A \equiv \lambda/v_{A,0}$. We use a non-uniform grid in the X -direction and a uniform grid in the Y -direction of 790×3000 zones. The minimum grid size in each direction is $\Delta x = 5 \times 10^{-3}$ and $\Delta y = 2.5 \times 10^{-2}$. A symmetric boundary condition is applied at $X = 0$ and $Y = 0$. A free boundary condition is imposed at $X = 50$ and $Y = 75$. We calculate numerical fluxes using the HLL method (Harten et al. 1983; Komissarov 2007) with an operator-splitting method. We use the implicit scheme to solve Ampere’s equation in order to maintain numerical stability when the electric resistivity is small (Palenzuela et al. 2009). The implicit scheme enables us to study magnetic reconnection with larger magnetic Reynolds number than previous studies.

Before presenting the numerical results, we estimate the speed of outflow driven by magnetic reconnection. Consider steady Sweet–Parker type magnetic reconnection in a diffusion region of length 2δ in the inflow direction and $2L$ in the outflow direction. Mass and energy conservation between the inflow and outflow give

$$\rho_{\text{in}} u_{\text{in}} 2L = \rho_{\text{out}} u_{\text{out}} 2\delta, \quad (2)$$

$$\begin{aligned} & \left[\left(\rho_{\text{in}} + \frac{\Gamma}{\Gamma-1} p_{\text{in}} \right) \gamma_{\text{in}} u_{\text{in}} + \frac{v_{\text{in}} B_{\text{in}}^2}{4\pi} \right] 2L \\ &= \left[\left(\rho_{\text{out}} + \frac{\Gamma}{\Gamma-1} p_{\text{out}} \right) \gamma_{\text{out}} u_{\text{out}} + \frac{v_{\text{out}} B_{\text{out}}^2}{4\pi} \right] 2\delta, \end{aligned} \quad (3)$$

where $\mathbf{u} = \gamma\mathbf{v}$ is the four velocity. The subscripts “in” and “out” indicate physical quantities in the inflow and outflow regions. Note that the ideal MHD ($\mathbf{E} = -\mathbf{v} \times \mathbf{B}$)

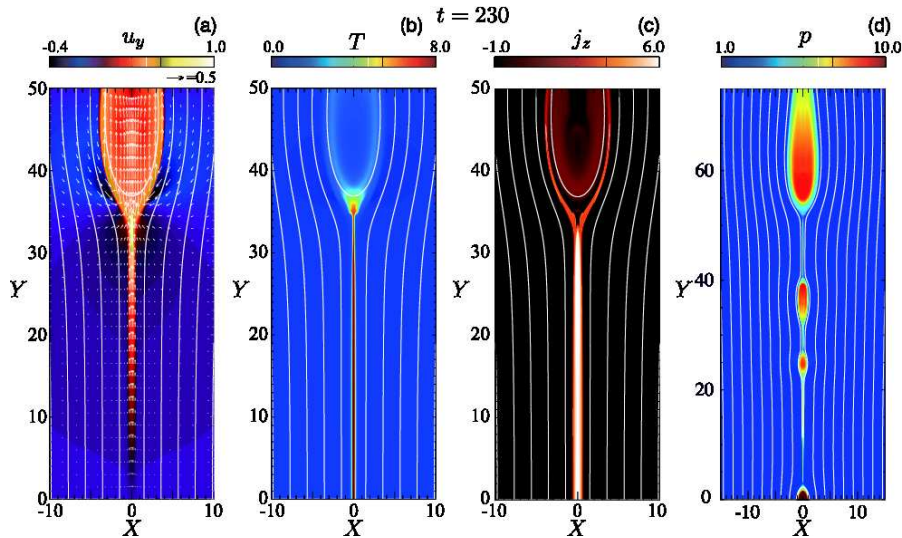


FIG. 1.— Snapshots at $t = 230$ of models B2R2 (Figs. 1a, 1b, and 1c) and B2R10 (Fig. 1d). The colors show (a) the outflow component of the four velocity (u_y), (b) the plasma temperature ($T = p/\rho$), (c) the electric current perpendicular to the X - Y plane (j_z), and (d) the gas pressure (p). The solid lines show the magnetic field lines. The arrows in Fig. 1a represent the velocity fields.

can describe both inflow and outflow plasmas because these flows are outside the diffusion region. Combining equations (2) and (3), we obtain

$$(1 + \sigma_{\text{in}} + h_{\text{in}}) \gamma_{\text{in}} = (1 + \sigma_{\text{out}} + h_{\text{out}}) \gamma_{\text{out}}, \quad (4)$$

where $h = \Gamma p / [(\Gamma - 1)\rho]$ is the specific enthalpy. This is similar to the Bernoulli equation that describes the conservation of the total enthalpy flux between the inflow and outflow. Assuming $\sigma_{\text{out}} \ll 1$, which is reasonable for the case of anti-parallel ($B_z = 0$) magnetic reconnection, we obtain

$$\gamma_{\text{out}} = \frac{1 + h_{\text{in}} + \sigma_{\text{in}}}{1 + h_{\text{out}}} \gamma_{\text{in}}. \quad (5)$$

If the magnetic energy is converted preferentially into kinetic energy ($h_{\text{in}} = h_{\text{out}}$), as was ideally assumed in Lyutikov & Uzdensky (2003), we obtain an upper limit of the outflow Lorentz factor γ_{max} ,

$$\gamma_{\text{max}} = \frac{1 + \sigma_{\text{in}} + h}{1 + h} \gamma_{\text{in}}. \quad (6)$$

γ_{max} listed in Table 1 is evaluated from an initial σ_{in} and h (we take $\gamma_{\text{in}} = 1$ in all models for numerical evaluation). Equation (6) reduces to $\gamma_{\text{max}} = (1 + \sigma_{\text{in}})\gamma_{\text{in}}$ when the thermal energy is negligible (see also equation 32 in Lyutikov & Uzdensky 2003). The outflow becomes super-Alfvénic in this case.

We stress that γ_{max} is the upper limit of the outflow Lorentz factor under the condition $h_{\text{in}} = h_{\text{out}}$. Since a part of the magnetic energy should be spent for plasma heating by ohmic dissipation, the enthalpy of the outflow is expected to increase and its Lorentz factor would be less than γ_{max} except in the ideal situation.

3. RESULTS

Figure 1 shows snapshots at $t = 230$ of model B2R2 (Figs. 1a, 1b, and 1c) and B2R10 (Fig. 1d). We focus here on Fig. 1a–1c (model B2R2), and will refer to Fig. 1d in § 4. The colors show (a) the outflow component of the four velocity (u_y), (b) plasma temperature ($T = p/\rho$), (c) electric current perpendicular to the X - Y plane (j_z), and (d) gas pressure (p). The

solid lines depict the magnetic field lines and the arrows represent the velocity fields. Following the initial perturbation, the magnetic field lines start to reconnect around the origin. As the reconnection proceeds, the current sheet is elongated along the $\pm Y$ -direction, indicating the formation of a Sweet–Parker current sheet. The plasma temperature inside the current sheet T_{cs} is almost uniform with a constant value ($\simeq 8.7T_{\text{in}}$). If adiabatic heating is the main process for plasma heating, T_{cs} would increase up to $\sim (\rho_{\text{cs}}/\rho_{\text{in}})^{1/3}T_{\text{in}} \simeq 1.22T_{\text{in}}$, where ρ_{cs} is the density inside the current sheet. Here we used the numerical result that $\rho_{\text{out}} \simeq \rho_{\text{cs}} \lesssim 1.8\rho_{\text{in}}$. Since the evaluated temperature is much less than the observed value, the plasma should be heated by ohmic dissipation rather than adiabatic heating in the diffusion region. The heated plasma is accelerated in the diffusion region along the $\pm Y$ -direction, resulting in the formation of hot outflows. The maximum outflow speed at this time is ~ 0.66 , which is slightly smaller than the Alfvén speed of the sheath plasma ($v_{A,0} \simeq 0.82$, discussed later). The reconnection outflows collide with a magnetic bubble (plasmoid) that originates in the initial Harris sheet. This causes the formation of reverse fast shocks around $Y \simeq 35$ outside the diffusion region. The plasma temperature near the plasmoid increases because of shock heating and the plasma expands. We note that a backflow ($v_y < 0$) structure forms around the plasmoid. Such backflow structures are also observed in Petschek type magnetic reconnection, which would be caused by the expansion of the plasmoid (Zenitani et al. 2010).

At this stage, the electric field around the reconnection region is well developed. The typical strength of the electric field near the reconnection point ($X \sim Y \sim 0$) is $E_z \simeq 1.0 \times 10^{-2}B_0$. In addition, an electric field ($E_z = v_y B_x$) is also induced near the plasmoid by the reconnected magnetic fields that are swept by the outflow and accumulate around $Y = 37$. Its maximum amplitude is $E_z \simeq 0.17B_0$, which is 17 times larger than that near the reconnection point. Such strong electric fields near plasmoids are also observed in particle-in-cell simulations (Jaroschek et al. 2004; Zenitani & Hoshino

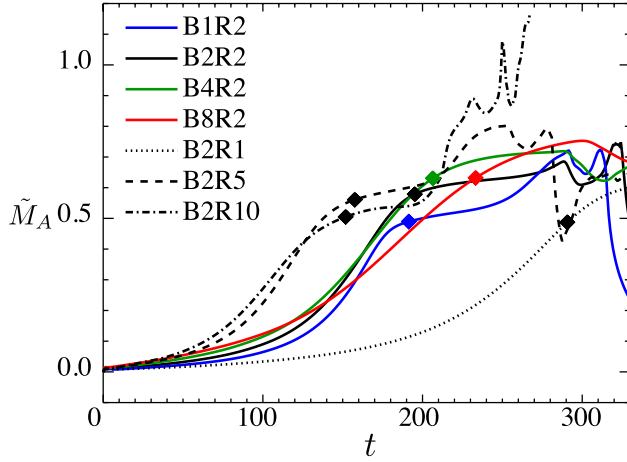


FIG. 2.— Time evolution of the maximum Alfvén four Mach number along $X = 0$ (\tilde{M}_A). The diamonds denote \tilde{M}_A at $t = t_{20}$.

2007) and two-fluid simulations (Zenitani et al. 2009b). These electric fields can generate high-energy particles (Hoshino 2005).

Figure 2 shows the time evolution of the maximum outflow component of the four velocity normalized by the Alfvén four speed in the sheath plasma along $X = 0$, $\tilde{M}_A \equiv \max[u_y(0, Y)]/u_{A,0}$. Each line shows the time evolution of a different model listed in Table 1. After the onset of magnetic reconnection, the outflow is accelerated along the Y -direction. Its acceleration decreases as the reconnection develops (e.g., $t \gtrsim 200$ for model B2R2). We note that \tilde{M}_A does not increase to the upper limit of the Alfvén Mach number $\tilde{M}_{A,\max} \equiv u_{\max}/u_{A,0}$ listed in Table 1 for each model, where $u_{\max} = \sqrt{\gamma_{\max}^2 - 1}$. This suggests that the magnetic energy is not efficiently converted into kinetic energy. The saturation values of \tilde{M}_A are independent of R_M , but weakly decrease as σ_0 increases.

In order to estimate the energy composition of inflow and outflow plasmas, we evaluate the magnetization parameter σ , specific enthalpy h and total specific enthalpy $1 + \sigma + h$ at $(X, Y) = (5, 0)$ for inflows and at $(X, Y) = (0, 20)$ for outflows, summarized in Table 1. These values are evaluated when the length of the current sheet L , which is defined by $j_z(0, L)/j_z(0, 0) = \alpha$, reaches $L = L_{20} \equiv 20$ (hereafter, we refer to this time as t_{20}). We take $\alpha = 0.5$ but the results are independent of α when $\alpha < 1$ since j_z is almost constant inside the current sheet and rapidly decreases at the edge of the current sheet. For example, the length of the current sheet of model B2R2 at $t = 230$ is $L = 33.3$ (see Fig. 1c).

Since we take $\sigma_0 > 1$, the inflow plasma is dominated by the magnetic energy ($1, h_{\text{in}} \ll \sigma_{\text{in}}$). In the outflow plasma, h_{out} is much larger than σ_{out} and unity, i.e., the thermal energy density dominates the rest mass and magnetic energy densities. Moreover, h_{out} is comparable to the total specific enthalpy of inflow ($1 + \sigma_{\text{in}} + h_{\text{in}}$). These results show that almost all the magnetic energy is converted into thermal energy due to joule heating. By using this fact, we can evaluate the outflow Lorentz factor from equation (5) as $\gamma_{\text{out}} \simeq 1$ in the condition $\gamma_{\text{in}} \simeq 1$. The outflow is not accelerated to a relativistic speed γ_{\max} . This result is consistent with that of the an-

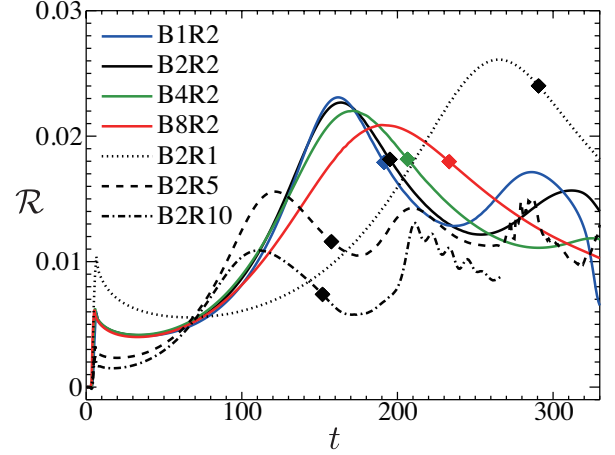


FIG. 3.— Time evolution of the reconnection rate (\mathcal{R}). The diamonds denote \mathcal{R} at $t = t_{20}$.

alytical work by Lyubarsky (2005). They concluded that the magnetic energy should be converted into thermal energy ($\sigma_{\text{in}} \simeq h_{\text{out}}$) to maintain the pressure balance across the current sheet. We confirmed that the current sheet reaches the pressure balance in the reconnection system, resulting in the formation of relativistically hot outflows. Such hot outflows cannot be accelerated to a relativistic speed γ_{\max} since the magnetic energy is spent in heating rather than acceleration. Moreover, a larger enthalpy ($h > 1$) leads to an increase in the plasma inertia in the relativistic regime (see equation 5). This also prevents the outflow from being accelerated. Sub-Alfvénic outflow is a natural outcome of relativistic Sweet–Parker reconnection because $\gamma_{\text{out}} = \sqrt{u_{\text{out}}^2 + 1}$ remains of order unity when $u_{A,0}$ increases with σ_0 . Thus, the Alfvén four Mach number decreases with increasing σ_0 in the relativistic regime. This conclusion is different from that for non-relativistic reconnection, in which the outflow speed reaches the Alfvén speed.

Figure 3 shows the time evolution of the reconnection rate $\mathcal{R} = -v_x/v_A$ at $(X, Y) = (5, 0)$. An initial rapid increase in the reconnection rate is caused by the initially imposed perturbation. After that, the reconnection rate gradually increases with time and reaches a maximum. Although the outflow speed is almost maintained at the saturated value, the reconnection rate decreases after passing its peak because the current sheet continues to elongate. Such an elongation of the current sheet is also observed in non-relativistic plasma (Tanuma et al. 2001). According to the non-relativistic theory, the aspect ratio of the Sweet–Parker current sheet is described by $\delta/L = \mathcal{R}$. Since the curvature radius of the initial magnetic field is infinite in the Harris sheet (i.e., uniform in the Y -direction), L tends to increase as the reconnection proceeds, resulting in a decrease in the reconnection rate.

Figure 4 shows the reconnection rate \mathcal{R} at $(X, Y) = (5, 0)$ as a function of R_M at $t = t_{20}$. The reconnection rate is almost independent of σ_0 for a fixed $R_M = 200$, while it decreases with R_M for a fixed $\sigma_0 = 10$. The solid line in this figure shows the relation $\mathcal{R} = S^{-1/2}$, obtained by Lyubarsky (2005) (see equation 8 in that paper), where $S \equiv 4\pi L_{20} v_{A,0}/\eta = R_M(L_{20}/\lambda)v_{A,0}$ is the Lundquist number. In this plot, we assumed $\sigma_0 = 10$ to evaluate the Lundquist number that weakly depends on

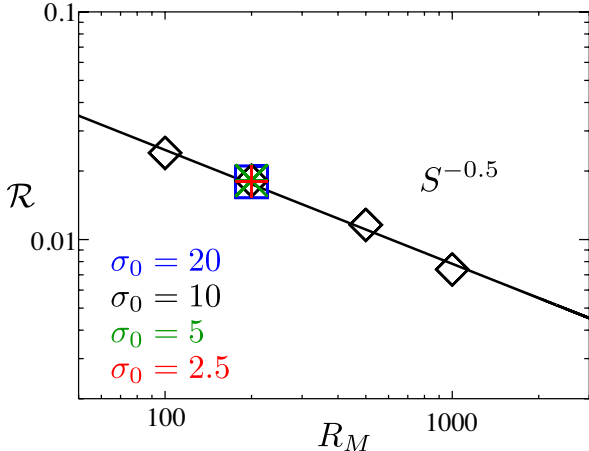


FIG. 4.— Reconnection rate (\mathcal{R}) as a function of magnetic Reynolds number (R_M). The reconnection rates are evaluated at $(X, Y) = (5, 0)$ when $t = t_{20}$. The black diamonds correspond to models of different R_M with the same $\sigma_0 = 10$, while the blue square, green asterisk, and red cross correspond to models of $\sigma_0 = 20, 5, 2.5$ with the same $R_M = 200$, respectively. The solid line shows $\mathcal{R} = S^{-0.5}$, where S is the Lundquist number, proportional to R_M .

σ_0 .

We found that the reconnection rate is well fitted by the steady model $\mathcal{R} = S^{-0.5}$, while the system is not exactly steady state. Although we are not sure why our time-dependent results follow those of the steady model, we also found the relation $t_L/t_{\text{rec}} = 0.5$ holds in the Sweet–Parker regime (e.g., $170 \lesssim t \lesssim 240$ for the model B2R2), where $t_{\text{rec}} = -(d \log \mathcal{R}/dt)^{-1}$ is the decreasing time of the reconnection rate and $t_L = (d \log L/dt)^{-1}$ is the increasing time of the length of the current sheet. This relation is obtained from $\mathcal{R} = S^{-0.5}$ by assuming that \mathcal{R} and L are time dependent. This means that the reconnection system evolves while maintaining the relation $\mathcal{R} = S^{-0.5}$.

Lyutikov & Uzdensky (2003) proposed that the reconnection rate is enhanced by the relativistic effect of the Lorentz contraction by a factor $\sqrt{\sigma_0}$ when $\sigma_0 \gg 1$ (see equation 39 in that paper). In our numerical models, however, such effects never become effective because of mildly relativistic outflow ($\gamma \simeq 1$), as discussed above. Therefore, the reconnection rate is almost independent of σ_0 and is described by $S^{-0.5}$. We conclude that relativistic Sweet–Parker reconnection is a slow process for energy conversion, as for non-relativistic plasma.

4. CONCLUSION AND DISCUSSION

We have developed a relativistic resistive magnetohydrodynamic (RRMHD) code that is applicable to plasmas with larger magnetic Reynolds numbers than possible in previous studies (Watanabe & Yokoyama 2006; Zenitani et al. 2010). We confirmed that the reconnection outflow does not accelerate to a relativistic speed

because the magnetic energy released by magnetic reconnection is spent on plasma heating rather than acceleration. The plasma heating results in increasing inertia, which also prevents the outflow from being accelerated. Since the Lorentz factor of the outflow is of order unity, the enhancement of the reconnection rate due to the Lorentz contraction is ineffective. Thus, the reconnection rate of the relativistic plasma obeys the relation $\mathcal{R} = S^{-0.5}$, which is the same as that for non-relativistic plasmas. We confirmed that this relation holds in the Sweet–Parker regime (i.e., $t_{10} \lesssim t \lesssim t_{30}$, where t_{10} and t_{30} are the time at which $L = 10$ and $L = 30$, respectively). These results are consistent with the theoretical prediction of Lyubarsky (2005).

We note that humps appear in the reconnection rate beyond the Sweet–Parker regime (see e.g., $t > 200$ for the model of B2R10 in Fig. 3). At this stage, we observed a growth of the tearing instability in the elongated current sheet (Fig. 1d, the model of B2R10). An increase in the reconnection rate following the instability is also observed in non-relativistic reconnection (Shibata & Tanuma 2001; Bhattacharjee et al. 2009; Cassak et al. 2009; Uzdensky et al. 2010; Huang & Bhattacharjee 2010). Once the tearing instability develops, the current sheet is disrupted and the system evolves to a non-steady state. A remarkable feature is that the increase in the outflow velocity coincides with the enhancement of the reconnection rate (e.g., $t > 200$ of model B2R10 in Figures 2 and 3). Although the reason for the acceleration is not yet clear, we speculate that the outflow is accelerated by the pressure gradient force. When the plasmoid created due to the tearing instability flows along the current sheet, the plasma in the current sheet is swept up by it. The subsequent outflow can then be accelerated by the pressure gradient force (see Fig. 1d). Since the plasma inertia $h \sim p/\rho$ decreases while it is accelerated by the pressure gradient force, the outflow speed might be ultra-relativistic $\gamma \gg 1$. In such cases, relativistic effects would facilitate the energy conversion in the reconnection process. These scenarios need to be verified through numerical simulations and will be reported in a subsequent paper.

We are grateful to the anonymous referee for improving our manuscript. We thank Ken-ichi Nishikawa, Ryoji Matsumoto, Shin-ya Nitta, Shu-ichiro Inutsuka, Tomoyuki Hanawa and Yosuke Mizuno, for helpful discussions. Part of this work was done while H. R. T. was visiting the University of Alabama in Huntsville. Support from the National Science Foundation is gratefully acknowledged. Numerical computations were carried out on Cray XT4 at the Center for Computational Astrophysics, CfCA, at the National Astronomical Observatory of Japan and on Fujitsu FX-1 at the JAXA Supercomputer System (JSS) at the Japan Aerospace Exploration Agency (JAXA).

REFERENCES

- Bessho, N. & Bhattacharjee, A. 2007, *Physics of Plasmas*, 14, 056503
- Bhattacharjee, A., Huang, Y., Yang, H., & Rogers, B. 2009, *Physics of Plasmas*, 16, 112102
- Biskamp, D. 1986, *Physics of Fluids*, 29, 1520
- Blackman, E. G. & Field, G. B. 1994, *Physical Review Letters*, 72, 494
- Cassak, P. A., Shay, M. A., & Drake, J. F. 2009, *Physics of Plasmas*, 16, 120702
- Di Matteo, T. 1998, *MNRAS*, 299, L15+

- Drenkhahn, G. 2002, *A&A*, 387, 714
- Gill, R. & Heyl, J. S. 2010, *MNRAS*, 407, 1926
- Harten, A., Lax, P. D., & van Leer, B. 1983, *SIAM Rev.*, 25, 35
- Hoshino, M. 2005, *Journal of Geophysical Research (Space Physics)*, 110, 10215
- Huang, Y. & Bhattacharjee, A. 2010, *Physics of Plasmas*, 17, 062104
- Jaroschek, C. H., Lesch, H., & Treumann, R. A. 2004, *ApJ*, 605, L9
- Kennel, C. F. & Coroniti, F. V. 1984, *ApJ*, 283, 710
- Kirk, J. G. & Skjæraasen, O. 2003, *ApJ*, 591, 366
- Komissarov, S. S. 2007, *MNRAS*, 382, 995
- Lyubarsky, Y. & Kirk, J. G. 2001, *ApJ*, 547, 437
- Lyubarsky, Y. E. 2003, *MNRAS*, 339, 765
- . 2005, *MNRAS*, 358, 113
- Lyutikov, M. 2006, *MNRAS*, 367, 1594
- Lyutikov, M. & Uzdensky, D. 2003, *ApJ*, 589, 893
- Masada, Y., Nagataki, S., Shibata, K., & Terasawa, T. 2010, *PASJ*, 62, 1093
- McKinney, J. C. & Uzdensky, D. A. 2010, *ArXiv e-prints*
- Palenzuela, C., Lehner, L., Reula, O., & Rezzolla, L. 2009, *MNRAS*, 394, 1727
- Priest, E. & Forbes, T. 2000, *Magnetic Reconnection (Magnetic Reconnection, by Eric Priest and Terry Forbes, pp. 612. ISBN 0521481791. Cambridge, UK: Cambridge University Press, June 2000.)*
- Shibata, K. & Tanuma, S. 2001, *Earth, Planets, and Space*, 53, 473
- Tanuma, S., Yokoyama, T., Kudoh, T., & Shibata, K. 2001, *ApJ*, 551, 312
- Tenbarge, J. M., Hazeltine, R. D., & Mahajan, S. M. 2010, *MNRAS*, 403, 335
- Tolstykh, Y. V., Semenov, V. S., Biernat, H. K., Heyn, M. F., & Penz, T. 2007, *Advances in Space Research*, 40, 1538
- Uzdensky, D. A., Loureiro, N. F., & Schekochihin, A. A. 2010, *Physical Review Letters*, 105, 235002
- Watanabe, N. & Yokoyama, T. 2006, *ApJ*, 647, L123
- Zenitani, S. & Hesse, M. 2008a, *ApJ*, 684, 1477
- . 2008b, *Physics of Plasmas*, 15, 022101
- Zenitani, S., Hesse, M., & Klimas, A. 2009a, *ApJ*, 705, 907
- . 2009b, *ApJ*, 696, 1385
- . 2010, *ApJ*, 716, L214
- Zenitani, S. & Hoshino, M. 2001, *ApJ*, 562, L63
- . 2007, *ApJ*, 670, 702
- Zhang, B. & Yan, H. 2011, *ApJ*, 726, 90